Elimination of Scan Blindness in Phased Array Antennas Using a Grounded-Dielectric EBG Material

Giacomo Donzelli, *Senior Member, IEEE*, Filippo Capolino, Stefano Boscolo, and Michele Midrio

***Abstract*—In printed phased arrays, scan blindness occurs when the propagation constant of a Floquet mode coincides with that of a mode supported by the homogeneous substrate, resulting in large input mismatch and in a propagating mode with complex propagation constant. In our study we analyze the possibility to replace a standard homogeneous dielectric substrate with a grounded dielectric EBG substrate to eliminate scan blindness. We present here the main idea for the design, the dispersion diagrams of a dielectric EBG material with metallic patches to show that there are no surface modes (waves guided by the structure with real propagation constant), and the active reflection coefficient and input impedance for various frequencies. Furthermore, at a chosen operating frequency the active reflection coefficient for the phased case indicates that there is no scan blindness effect.**

***Index Terms*—Arrays, band gap, dielectric resonators, electromagnetic bandgap (EBG) materials, phased arrays, scan blindness.**

I. Introduction

PERIODIC electromagnetic bandgap (EBG) materials have been used recently to modify the radiation pattern and other characteristics of sources located near or within it. The radiation performances of arrays on standard dielectric substrates are impaired by the surface waves, supported by the substrate, that affect the radiation efficiency and increase the interelement coupling. Performances are also constrained by the appearance of scan blindness phenomena that is common for printed arrays on dielectric substrate [1], [2]. Scan blindness limits the scan range because of a large input mismatch at a certain scanning angle when a spatial harmonic of the periodic array matches the phase propagation of a mode supported by the substrate. At this particular blind scanning angle, the mode of the periodic structure, excited by the phased array, becomes complex because the array is "designed" to radiate and thus one Floquet harmonic of the guided mode appears into the visible range. When this occurs, the field is both propagating and attenuating along the array plane, resulting in power loss through the substrate and in a large input mismatch. Recently, some EBG substrates have been investigated to eliminate this problem [3]–[6], but none of them resembles the one presented here.

In this letter, a new grounded dielectric EBG material is used as an antenna substrate and as a radiating array with the aim of avoiding scan blindness. The main idea is that of designing the whole structure, i.e., the patterned substrate plus the patches, so that it has a forbidden gap at the working frequency *and* no scan blindness. This way, no guided waves will be supported by the structure at the desired frequency and the power will not be lost in surface waves that would be excited by the array-truncation effects or by the rapid variation, from element to element, of the excitation. Not only guided waves (surface waves) should be absent, in order not to have scan blindness the periodic structure should *also* not support leaky waves that cannot be detected with a simple Brillouin dispersion diagram for real wavenumbers.

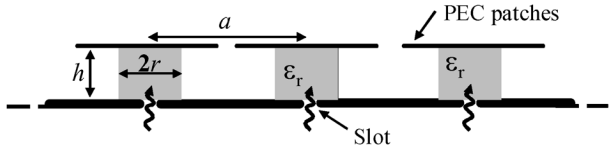

Fig. 1. Lateral view of the array of antennas consisting of metallic patches on the EBG substrate made of a square lattice of dielectric rods in air over a ground plane. The structure acts both as a radiating array and an EBG substrate. Each element is fed by a slot on the ground plane.

We do not simply design a patterned dielectric substrate with a proper band-gap. Rather, the novelty consists in designing a structure in which both the patterned substrate and the patches concur to create the gap. This has a major advantage. Indeed, if one designs first a patterned substrate with bandgap, and then prints antennas on it, propagation of surface waves can be suppressed only if antennas are placed quite far apart the one from the others because a few periods of the lattice are required in order for the waves to feel the resonances induced by the patterned substrate, and being blocked. On the contrary, if the ensemble of the patterned substrate and the patches is designed at the same time with distance between antennas coincident with the lattice pitch, the bandgap performances are quite different from those of a patterned EBG substrate alone. Also, this way, the antennas are more closely packed, and appearance of grating lobes can be avoided because of the reduced spacing between the radiating elements. The proposed structure also has the advantage of providing wider bandwidth (10 dB bandwidth equal to 4.9% in this case, without any particular design or trying to optimize it) than standard patches since each radiating element consists of the whole three dimensional dielectric rod with metallic patch on top.

The letter flows as follows. We first present and discuss the surface-wave bandgap properties of the EBG material that consists of a periodic arrangement of alumina rods on top of a ground plane. A squared metallic patch is located on top of each dielectric rod. Note that both metallic patches and dielectric rod constitute the EBG substrate (Figs. 1 and 2), and the

Manuscript received December 8, 2005; revised January 12, 2007.

G. Donzelli and F. Capolino are with the Department of Information Engineering, University of Siena, Siena, Italy (e-mail: capolino@dii.unisi.it).

S. Boscolo and M. Midrio are with the Department of Electric Engineering, University of Udine, Udine, Italy.

Digital Object Identifier 10.1109/LAWP.2007.892043

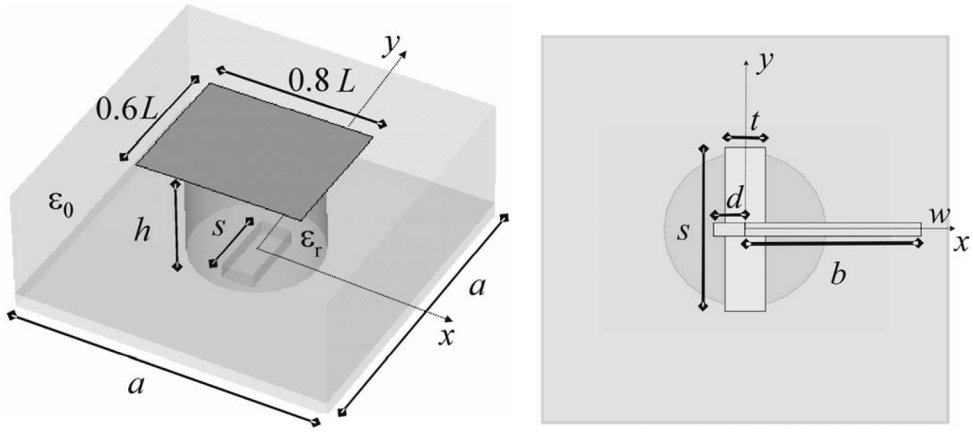

(*a*) (*b*)

Fig. 2. (a) Three-dimensional view of a periodic cell. (b) Bottom view of the periodic cell with an aperture-coupled microstrip feed. Dimensions (in mm): rod radius $r = 2, a = 10, h = 3.95, L = 9, s = 4.2, t = 1, d = 0.78, b = 4.3, w = 0.36$, microstrip substrate thickness $= 0.258$. Furthermore, rod permittivity $\varepsilon_r = 9$, microstrip substrate permittivity $\varepsilon_r = 2.1$.

patches have the role to widen the bandgap. Furthermore, each metallic patch and dielectric rod also constitute a radiating element. Next, a phased array of such radiating elements is fed by slots to analyze the radiation pattern of each element. Then, a microstrip is used to excite each slot and we show how these radiators can be matched to a feeding line and we analyze the active reflection coefficient for various scan angles along the E- and H-plane. Numerical simulations show that there is no blind angle in both the E- and H-plane, since for all scanning angles in these planes the large mismatch typical of scan blindness does not occur.

II. Design and Numerical Results

In Fig. 1, we show the lateral view of the array of patch antennas on the EBG substrate made of a square lattice of dielectric rods in air over a ground plane. Three main parameters determine the performance of our structure: r/a with a the period of the EBG material and r the radius of the dielectric rods, as well as the height h and the relative permittivity ε_r of the rods. A metallic rectangular patch is placed on top of each rod with dimensions $0.8L \times 0.6L$, where L is a tuning parameter used to optimize the radiation pattern and the input impedance. Each antenna consisting of a dielectric rod and a metallic patch is fed via a microstrip-excited slot on the ground plane (Figs. 1 and 2).

Each dielectric rod acts as a resonator in the vertical direction [7], and resonance is achieved by setting the rods height equal to $h \approx \lambda_r/2$, where $\lambda_r = \lambda_0/\sqrt{\varepsilon_r}$ and λ_0 is the free space wavelength. Various simulations show that the size of the metallic patch does not significantly affect the resonance condition. Furthermore, at the operating frequency, the period a is smaller than $\lambda_0/2$ to avoid grating lobes.

As we aim at eliminating scan blindness *and* suppressing propagation of guided waves (still keeping the vertical resonant condition $h \approx \lambda_r/2$), the structure needs to have a transverse bandgap at the operating frequency of $f = 12.68$ GHz. That is, no modal propagation should be allowed in the plane containing the array that could either lower the efficiency (guided waves with real propagation constant) or cause mismatch (scan

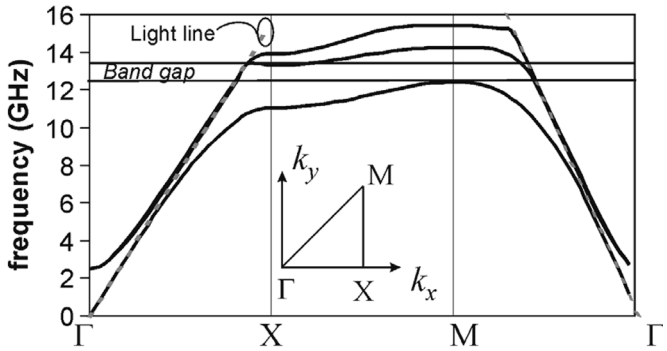

Fig. 3. Dispersion diagram for modal propagation in the grounded EBG material made of dielectric rods and metallic patches. Dimensions are given in the caption of Fig. 2. On the horizontal axis, $\Gamma(k_x = k_y = 0), \mathrm{X}(k_x = \pi/a, k_y = 0)$, an $M(k_x = k_y = \pi/a)$, where k_x and k_y are the propagation wavenumbers along x and y, respectively, denote the extremes of the irreducible Brillouin zone.

blindness, caused by a leaky wave). For instance, if the dielectric rods are made of alumina with $\varepsilon_r = 9$, this can be obtained with following choice of parameters: $r/a = 0.2, h = 3.95$ mm, and the patch size $0.8L \times 0.6L$ with $L = 9$ mm. Indeed, as shown in Fig. 3, a full bandgap is obtained in the frequency range $12.42 < f\ (\mathrm{GHz}) < 13.36$. For these calculations, the slots have been short circuited. All the numerical results are obtained with the commercial software CST Microwave Studio by modeling a single array-element with periodic boundary conditions. We have noticed that the metallic patches have a remarkable influence on the location of the bandgap and thus they need to be included for the calculation of the dispersion diagram. Moreover, as expected, the difference between the dispersion curves in the absence and in the presence of the metallic patch tends to increase when using larger patches. We have performed a thorough analysis of the dispersion curves that are obtained when varying the parameter L which sets the patch size (Fig. 2). For the sake of brevity, we do not report here all the graphs, and we only state the main results we have obtained. We have observed that the bandwidth of the gap widens when the patch size increases. Vice versa, the radiation pattern

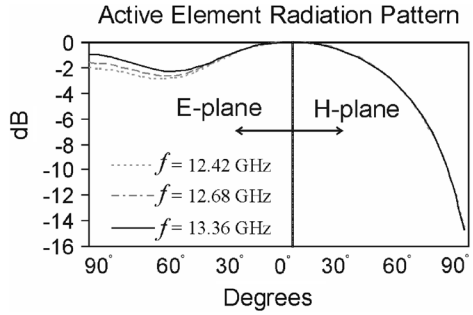

Fig. 4. Normalized active radiation pattern along the E- and H-plane of a single array element shown in Fig. 2(a), extracted from a periodic arrangement, with all the array elements excited.

of the field radiated by the patch tends to be more regular (without deep maxima and minima) when the patch size decreases. Most likely, this depends on the fact that a small patch lie entirely within the high-index rods, whilst a large patch would cover both the high-index region and the low-index one. In this case, currents on the patch exhibit rather curly lines on a larger surface, which in turns produce more irregular radiation patterns. Thus, the chosen parameter $L = 9$ mm is the result of a compromise between these two trends.

Fig. 4 shows the active radiation patterns on the E- and H-plane of a *single* radiating element at one frequency $f = 12.68$ GHz within the bandgap, and at its lower and upper frequency edges, $f = 12.42$ and $f = 13.36$ GHz, respectively. They are computed by CST Microwave Studio that simulates the whole infinite periodic structure by using periodic boundary conditions, and successively extracts the radiation by the aperture field of a single array element. Note that the radiation pattern does not change significantly at the three frequencies considered. The feed of each array element consists of a slot on the ground plane located and centred under the dielectric rod, with dimensions $s = 4.2$ mm and $t = 1$ mm, excited by a microstrip with width $w = 0.36$ mm, and printed on a dielectric substrate with thickness equal to 0.258 mm and relative dielectric permittivity $\varepsilon_s = 2.1$ [Fig. 2(b)]. At the bandgap center frequency $f = 12.68$ GHz, the microstrip has a characteristic impedance $Z_0 = 80\ \Omega$. The matching has been designed for broadside radiation (pointing angle $\theta_0 = 0°$) at $f = 12.68$ GHz with a stub length $d = 0.78$ mm. Therefore, all the elements are excited in phase, and this is automatically assumed when using periodic boundary conditions that enforce $\theta_0 = 0°$. In our case, the E-plane is the plane aligned along the longer patch dimension, and orthogonal to the slot, while the H-plane is along the smaller patch dimension and parallel to the slot longer dimension.

Fig. 5 shows the active reflection coefficient as well as the real and imaginary part of the active input impedance at a microstrip port 4.3 mm away from the center of the slot, for an equally phased array (broadside radiation). Notice that the antenna input 10 dB-bandwidth for broadside radiation extends from 12.38 to 13 GHz, which represents the 4.9% of the operating frequency $f = 12.68$ GHz.

The active reflection coefficient of the array at the frequency of 12.68 GHz is plotted in Fig. 6 for the phased case, versus

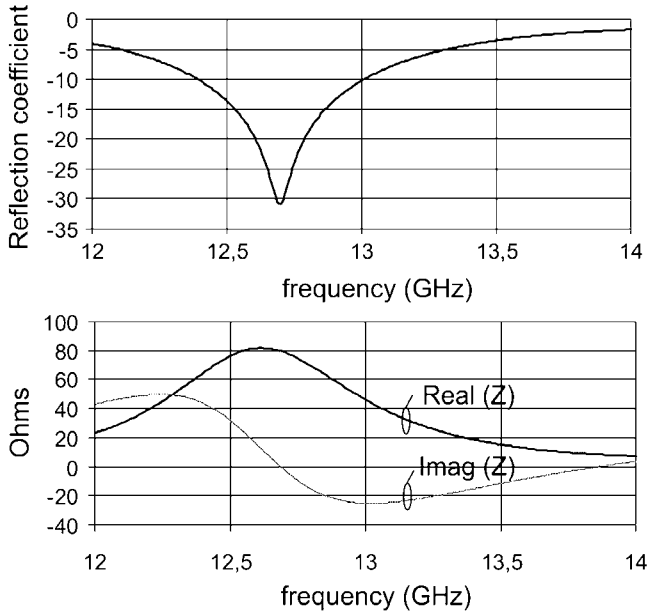

Fig. 5. Active reflection coefficient and active input impedance Z, for the element shown in Fig. 2, fed by a slot excited by a microstrip with a stub.

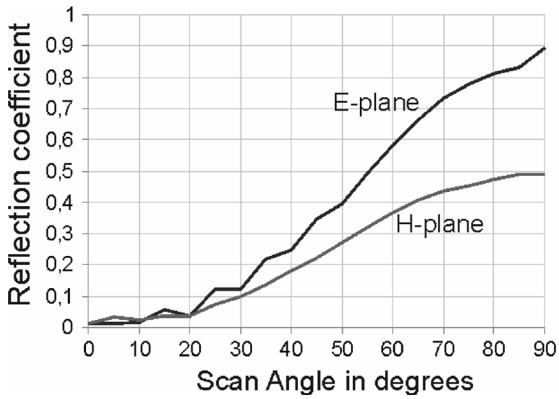

Fig. 6. Active reflection coefficient for the phased array antenna whose single element is shown in Fig. 2(a), when the beam is scanned along the E- and H-plane, at a frequency $f = 12.68$ GHz.

beam scan angle θ_0 along the E- and H-planes. The scan angle θ_0 is imposed by the array element phasing and not necessarily corresponds to the actual pointing angle of the beam, especially for large angles, as usually occurs in phased arrays because of mismatch and of the rapid variation of the array-element pattern for large observation angles. The active reflection coefficient in Fig. 6 never reaches 0 dB thus showing that the scan blindness effect can be avoided with the use of this combined EBG-antenna substrate. Active reflection coefficients that show scan blindness can be seen in ([1, Figs. 3–7], ([2 ,Figs. 3–4], ([4, Figs. 4–7]), ([6, Fig. 5]).

III. Conclusion

Numerical results have shown that propagation of surface waves (guided waves with real propagation constant) can be suppressed in a properly designed periodic array. Furthermore,

a numerical prediction of the active reflection coefficient indicates that in the proposed array geometry scan blindness does not occurr for all phasing angles along the E- and H-planes.

Other few array solutions involving different gemetries of bandgap substrates or surfaces [3]–[6] or other types of array element antennas such as cavity backed elements, have been proposed in the past. This study constitutes an alternative design for a phased array that does not exhibit scan blindness and does not support surface waves, with element distances less than half free-space wavelength and thus without grating lobes. Furthermore, since the EBG elements act like dielectric resonator antennas [7], it is easy to obtain a reasonable large input bandwidth.

Advantages with respect to other solutions deserve further investigation and thus showing them is not the purpouse of this Letter. However, possibly they rely on the relative simplicity of the design, which flows as follows. As a first step, once the operating frequency is given, the height of the rods is set, as the rods need to operate as half-wavelength dielectric cavities. Then, the dimensions of the patch may be set so to match the required radiation pattern. At this stage, the ratio between the rods diameter and period, i.e., the filling factor, remains to be determined, and this is done by requiring that a bandgap opens up at the working frequency. The input impendace is then mainly determined by the slot width and length and microstrip line.

The proposed geometry has the advantage that each element is radiating and thus the numerical cost for computing the radiation and input characteristics in an infinite periodic arrangement is rather limited because the period of the radiating structure coincides with that of the EBG substrate.

REFERENCES

[1] D. M. Pozar and D. H. Schaubert, "Scan blindness in infinite phased arrays of printed dipoles," *IEEE Trans. Antennas Propag.*, vol. 32, pp. 602–610, Jun. 1984.

[2] ——, "Analysis of an infinite array of rectangular microstrip patches with idealized probe feeds," *IEEE Trans. Antennas Propag.*, vol. 32, pp. 1101–1107, Oct. 1984.

[3] Z. Iluz, R. Shavit, and R. Bauer, "Microstrip antenna phased array with electromagnetic bandgap substrate," *IEEE Trans. Antennas Propag.*, vol. 52, no. 6, pp. 1446–1453, Jun. 2004.

[4] L. Zhang, J. Castaneda, and N. G. Alexopoulos, "Scan blindness free phased array design using PBG materials," *IEEE Trans. Antennas Propag.*, vol. 52, no. 8, pp. 2000–2007, Aug. 2004.

[5] J. C. I. Galarregui, I. Ederra, R. G. Garcia, and P. de Maagt, "Circularly polarized phase array on a high dielectric constant EBG substrate," in *JINA 2004 (J. Int. Nice sur les Antennes)*, Nice, France, Nov. 8–10, 2004.

[6] Y. Fu and N. Yuan, "Elimination of scan blindness in phased array of microstrip patches using electromagnetic bandgap materials," *IEEE Antennas Wireless Propag. Lett.*, vol. 3, pp. 63–65, 2004.

[7] S. A. Long, M. W. McAllister, and L. C. Shen, "The resonator cylindrical dielectric cavity antenna," *IEEE Trans. Antennas Propag.*, vol. 31, no. 3, pp. 406–412, May 1983.